Detection, biophysical effects, and toxicity of polystyrene nanoparticles to the cnidarian Hydra attenuata

Auclair, Joëlle; Quinn, Brian; Peyrot, Caroline; Wilkinson, Kevin James; Gagné, François

Published in:
Environmental Science and Pollution Research

DOI:
10.1007/s11356-020-07728-1

Published: 23/01/2020

Document Version
Peer reviewed version

Detection, biophysical effects and toxicity of polystyrene nanoparticles to the cnidarian *Hydra attenuata*

Joëlle Auclair, Brian Quinn, Caroline Peyrot, Kevin JamesWilkinson, François Gagné*

1. Aquatic Contaminants Research Division, Environment and Climate Change Canada, 105 McGill, Montréal, Québec, Canada H2Y 2E7. Francois.gagne@canada.ca 2. School of Health and Life Sciences, University of the West of Scotland, Paisley, Scotland, United Kingdom PA1 2BE. 3. Chemistry Department, Montreal University, Montréal, Québec, Canada H2V 2B8.

* Corresponding author: François Gagné: francois.gagne@canada.ca

Abstract

The occurrence of nanoplastic particles (NPs) in the environment has raised concerns about the ecotoxicological risk to aquatic ecosystems. The purpose of this study was to examine the bioavailability and toxicity of 50 and 100 nm transparent polystyrene NPs to the cnidarian *Hydra attenuata*. The hydra were exposed to increasing concentrations of 50 and 100 nm NPs (1.25, 2.5, 5, 10, 20, 40 and 80 mg/L) for 96 h at 20^{o}C followed by a 24h-depuration step. Hydra were analysed for morphological changes, bioaccumulation of NPs using a novel assay for polystyrene NPs, oxidative stress (lipid peroxidation), polar lipids, lipid-like liquid crystals (LCs) and viscosity changes in the post-mitochondrial fraction. The results revealed that the organisms accumulated detectable amounts of NP in a concentration dependent manner for both the 50 and 100 nm NP that persisted after 24 h in clean media. Changes in morphology were observed with a 50% effect concentration of 3.6 and 18 mg/L for the 50 and 100 nm diameter NPs respectively. However based on the particle density, the 100 nm proved to be 1.7 times more toxic than the 50 nm NPs. Exposure to NPs led to decreased biomass, lipid peroxidation (LPO), increased polar lipids levels, viscosity and formation of LCs at the intracellular level. In the more toxic NP (100 nm), NPs in tissues were correlated with LCs, polar lipids and LPO levels. It appears that the formation of organized LCs and polar lipids of NPs in cells was involved with NPs toxicity and could represent a yet unidentified, detoxifying/bioactivation mechanism against colloidal plastics in cells. In conclusion, NPs are bioavailable to hydra and lead to LPO and lipid mobilisation in hydra. The capacity of increasing lipid mobilization and LCs could determine the size-dependence toxicity of NPs.

Key words: nanoplastics, polystyrene, hydra, oxidative stress, neutral lipids.

Introduction

Plastic products are ubiquitous in the environment as they permeate many aspects of our daily lives. They can be found in various products such as coatings, cosmetics, wiring, packaging, film covers, bags and miscellaneous containers (Al-Salem et al., 2009). Although many plastics are recycled, they are unfortunately still found in most water bodies including rivers and oceans

persisting for decades in the environment. Plastic particles could degrade in the environment from abiotic (physical abrasion) and biotic factors leading to microplastics (operationally defined as materials between 1 µm to 5 mm) and nanoplastics (NPs; 1 to 100 nm) (Lambert and Wagner, 2016). The long-term degradation of plastic materials will lead to staggering quantities of NPs in the environment. Polystyrene-based plastics are one of the most abundant forms of plastics representing circa 10% of total plastic production (Verschcoor et al., 2017) and can remain in the environment for hundreds of years (Ho et al., 2018). Although microplastic materials can clog and damage the digestive system and skin in birds and aquatic animals, the small size of NPs makes them permeable to tissues and cells whereas they can accumulate and produce unknown effects at the intracellular/macromolecular levels. Indeed, internalized NPs were shown to damage cells by apoptosis, protein denaturation/fibrillation and the formation of organized lipophilic liquid crystals (LCs) in cells (Colvin and Kulinowski, 2007; Wang et al., 2013; Gagné et al., 2019a). Although several studies can be found on the effects of NPs in marine organisms, there are a limited number of studies on the toxicity of NPs in freshwater invertebrates.

The freshwater hydranth *Hydra attenuata* is commonly found in freshwater ecosystems and is a well-recognized test organisms in aquatic toxicity studies (Blaise and Kusui, 1997; Pascoe et al., 2003; Quinn et al., 2012). The hydra is a simple organism composed of a tube-like structure, with a foot attaching to a solid substrate and a head composed of 4-6 long tentacles for food capture. The toxic intensity (reversible sub-lethal to irreversible lethal effects) can be conveniently observed trough a stereomicroscope by a series of morphological changes such as antennae shortening, loss of antennae and compressed tube. More recently, the hydra was used to examine the toxicity of both microplastics (Murphy and Quinn, 2018) and nanoplastics (Gagné et al, 2019b). Hydra were able to ingest small microplastics fragments from face wash soaps that

compromised feeding activity and displayed sub-lethal stress by regression of antenna. These studies revealed that microplastics could reduce feeding activity whereas NPs could significantly induce reversible morphological changes and increase polar lipids levels in hydra. In the case of polystyrene NPs, the styrene-based surface provides a hydrophobic environment (aryl benzene) which could induce strong hydrophobic interactions given the high surface area of nanoparticles. It is hypothesized that the introduction of the hydrophobic surface of NPs could elicit changes on lipid mobilization and other macromolecules such as less polar proteins/peptides at the surface of the NPs.

The purpose of this study was therefore to examine the bioavailability and toxicity of 50 and 100 nm polystyrene NPs in *Hydra attenuata*. The bioavailability of NPs was determined by a novel fluorescent probe methodology. Toxicity effects were determined by both morphological changes and sublethal biomarkers. The latter consisted in changes in lipid peroxidation, polar lipid levels, microviscosity changes and the formation of anisotropic LCs. The mode of action based on hydrophobic interactions of NPs was examined in hydra exposed to NPs.

Materials and Methods

Preparation and exposure of NPs to hydra

Transparent, unlabeled polystyrene nanoplastics (NP) of 50 and 100 nm diameter were obtained from Polyscience Inc (USA). The hydra were maintained in a media consisting of 1 mM $CaCl_2$ and 0.5 mM TES (N-tris [hydroxymethyl]methyl 1-2- aminoethanesulfonic acid), pH 7.0 at 20^{o}C as previously described (Blaise and Kusui, 1997) and were fed each day with preparations of live *Artemia salina* brine shrimps. Exposure tests were conducted in 12-well microplates with three animals placed in each well (n=9 hydra per treatment) containing 4 mL of media. The NP suspension was prepared at 0.5 g/L in MilliQ water to prevent aggregation, with the final dilutions

prepared in hydra media. The size distribution of these NPs were examined in MilliQ water and in the incubation media using dynamic light scatter instrument with an operating laser at 532 nm (Mobius Instrument, Wyatt Technologies, Santa Barbara, CA, USA). Unexposed hydra maintained in culture media only served as controls. The exposure concentrations used were 0, 1.25, 2.5, 5, 10, 20, 40 and 80 mg/L corresponding to 0.32, 0.64, 1.29, 2.57, 5.15, 1.03, 2.06 $x10^{12}$ nanoparticles/L for the 50 nm NP and 0.04, 0.079, 0.159, 0.318, 0.636, 1.27, and 2.54 $x10^{11}$ nanoparticles/L for 100 nm NP respectively. Hence, on a mass basis, 50 nm NP contains 8 times more particles than the 100 nm NP. The selected concentration were chosen to attain a lethal concentration which was in ppm range. These concentrations are not necessarily environmentally realistic but could be attained in a spillage situation (e.g. sediments contaminated by miscellaneous plastics compounds released by a nearby industry or source).

After the exposure period (96 h), changes in hydra morphology were determined under a 6 x stereomicroscope based on the Wilby scale (Wilby, 1989). Normal control animals maintained a normal size with long and slender tentacles; sub-lethal (reversible) effects consisting of hydra showing clubbed or reduced tentacles length and lethal (irreversible) effects consisting in shrunken hydra at the tulip or disintegrated stages. Representative examples for each morphological changes are presented in Figure 1. The number of hydra with morphological changes was the variable used to estimate the 50 % effects concentration (EC50) and the 50% lethal concentration (LC50). The positive control consisted of $ZnSO_4$ (LC50 of 1 mg/L; 0.7-1.3 mg/L 95% confidence interval) which was used for quality assurance control. A subset of hydra at the low exposure group and controls (0, 1.25, 2.5 and 5 mg/L) were allowed to depurate in clean media for 24 h before freezing to determine the elimination potential of the NPs and persistence of toxicity. At the end of the morphological assessment, the hydra media was removed from the wells, the hydra washed in 1

mL of media, detached and suspended in 250 µL homogenisation buffer consisting of 50 mM NaCl containing 10 mM Hepes-NaOH, pH 7.4, 0.1 mM dithiothreitol and 0.1 µg/mL apoprotinin (protease inhibitor). Samples were stored at -85^{o}C for NP uptake and biomarker analyses. The hydra were homogenized using an hand-held pestle tissue grinder (Canlab, ON, Canada). The homogenate was allowed to settle on ice for 30 min. Total protein contents in the homogenate were determined using the Coomassie Brillant Blue methodology in clear 96-well microplates (Bradford, 1976). Serum bovine albumin was used for calibration.

Detection of NPs in hydra

Detection of polystyrene NPs was performed using the molecular rotor probe methodology (Gagné, 2019). The probe consisted of a 10 mM stock solution of 9-(dicyanovinyl)-julolidine (DCVJ) in ethanol, diluted to 10 µM in MilliQ water on the day of analysis. For the assay, 20 µL of the homogenate was mixed with 180 µL of 10 µM of DCVJ probe in 96-well dark microplate. Fluorescence was measured at 620 nm and 520 nm emission at 450 nm excitation for NP and viscosity measurements respectively. Standard solutions of polystyrene NPs at 50 nm diameter (0.05 and 0.1 µg/mL) were prepared for instrument calibration where 1 RFU corresponds to 1 µg/mL NP. The data weas expressed a relative fluorescent units-RFU /mg proteins.

Early biological effects of NPs

The viscosity of the homogenate was determined by the DCVJ probe at the reported emission wavelength (520 nm emission; 450 nm excitation) for viscosity assessment (Haidekker et al., 2001). The viscosity of a media could be defined as the resistance of molecules to movement in space at a given temperature. The DCVJ is a molecular rotor probe where energy is dispersed by either by kinetic rotation or by fluorescence. As the viscosity increases, rotation is limited and

fluorescence increases to compensate this restriction. A volume of 20 µL of the homogenate was mixed with 180 µL of DCVJ probe as described above. Standard solutions of glycerol were used for calibration for instrument calibration where 1 RFU corresponds to 10 µg/mL of glycerol. The formation of dissipative structures such as liquid crystals (LCs) in the homogenate was determined using fluorescence polarisation spectroscopy (Gagné et al., 2019a). The hydrophobic fluorescent octadecyl ester (FOE) probe was used to detect the formation of LCs in hydra exposed to NPs. The FOE probe was dissolved in dimethylsulfoxide at 1 mM concentration and kept at room temperature in the dark. On the day of analysis, the FOE probe was diluted at 10 µM in 10 mM KH_2PO_4 and Hepes-NaOH, pH 7.4, containing 140 mM NaCl. A 20 µL volume of the homogenate was mixed with 200 µL of 10 µM FOE and fluorescence polarization was determined at 485 nm excitation and 520 nm emission. Fluorescence polarisation was calculated by determining the ratio between the perpendicular and parallel direction of the emission signal (perpendicular-parallel fluorescence / perpendicular+parallel fluorescence) using dichroic mirrors (Synergy-4, Biotek instrument, USA). Standard solutions of 50 nm NPs (0.05, 0.1 and 0.15 µg/mL) were prepared since the polarization was shown to be concentration dependent in the presence of homogenate extract (Gagné et al. 2019a). The fluorescence polarization data were imported to an Excel Spreadsheet and analysed with SYSTAT software (version 13.2; USA). Fluorescence polarization was measured in the same of amount of homogenate proteins (10 µg/mL).

Lipid peroxidation (LPO) was determined in hydra homogenates using the thiobarbituric acid method (Gagné, 2014) using a miniaturized adaptation for small volumes in 384-well microplates. A volume of 10 µL of the homogenate was mixed with 20 µL of 10% trichloroacetic acid containing 1mM FeSO4 and 10 µL of 0.7% thiobarbituric acid in 384 wells dark microplates. The mixture was placed at 75 °C for 10 min, cooled at room temperature before taking fluorescence

measurements. Fluorescence readings were taken at 540 nm excitation and 600 nm emission using standard solutions of tetramethoxypropane (stabilized form of malonaldehyde) for calibration in the blank media (homogenization buffer only). Results were expressed as μg thiobarbituric acid reactants (TBARS)/mg total proteins in the homogenate.

The polar fraction of lipids in the homogenate was determined using the Nile red methodology (Greenspan and Fowler, 1985). Nile red was prepared as 10 mM in methanol and diluted to 10 μM in MilliQ water. A 20 μL volume of the homogenate was mixed with 180 μL of Nile red probe. After 10 min, fluorescence was measured at 500 nm excitation and 650 nm emission (Synergy 4, Biotek microplate reader, USA). Instrument calibration was achieved with standard solutions of Tween-20 (0.01 to 0.05%). Data was expressed as relative fluorescence units (RFU)/mg proteins in the homogenate.

Data analysis

The study design examines the bioavailability and toxicity in hydra exposed to the 7 increasing concentrations of 50 and 100 nm NPs. The 96-h toxicity (50 % lethal concentration) was determined using the Spearman-Karber method and the 96-h sub-lethal effect concentration (50% effect concentration) using the Log-logit method (Finney, 1964). Data normality and homogeneity of variance were verified using the Shapiro-Wilk and Bartlett tests respectively. The data was analysed using analysis of variance and critical differences between the controls and exposure concentrations were determined using the Least Square Difference test. The trends between the data were also analyzed using Pearson-moment correlation and principal component analysis. All tests were performed using the SYSTAT software (version 13). Significance was set at $p < 0.05$.

Results

On a mass basis, the stock solutions of 50 nm polystyrene NPs (6.7 x 10^{14} particles/mL) contained 8 times more particles than the 100 nm NPs (8.3 x10^{13} particles/mL). The size distribution of the NPs were analyzed using dynamic light scattering and revealed that the NPs were distributed at the specific diameter (50 and 100 nm) and did not form aggregates. The levels of NPs was determined using the DCVJ probe methodology in hydra exposed for 96h to the NPs and following a 24h depuration with the low concentrations (1.25-5 mg/L) and controls (Figure 2). The analysis revealed that hydra accumulated both sizes of NPs in a concentration dependent manner. For the 50 nm NPs, the NPs were detected at the lowest concentration (1.25 mg/L) which persisted after a 24h depuration period. For the 100 nm, the NPs in hydra at the lowest concentration were more abundant on a mass basis than the 50 nm NPs suggesting that the 100 nm NPs were more bioavailable than 50 nm NP. Indeed, hydra accumulated 24 times more NPs with the 100 nm diameter size even though they were 8 times less abundant than the 50 nm NPs. Although the probe was shown to react with NPs in vitro, we could not determine if a small fraction was still attached on the tentacles and in the gut although the hydra were washed. This is why a 24-depuration period was done to determine if the NPs in Hydra could be removed in clean media (where most of the NPs were still present at that time). The toxicity of the hydra was examined based on the characteristic morphological changes (Figure 1). Although no mortality was observed based on the complete regression/destruction of the hydra, the EC50 based on the shortened morphology of the hydra was 3.6 (9.22 x 10^{11} particles/mL) and 18.4 mg/L (5.81x10^{11} particles/mL) for the 50 and 100 nm NPs (Table 1). Hence, despite having a higher EC50, the 100 nm NPs were circa 1.7 times more toxic than the 50 nm on a particle basis. The biomass of hydra was also significantly reduced at 14 (3.58 x 10^{12} particles/mL) and 28 mg/L (8.8 x 10^{11}

196 particles/mL) for the 50 and 100 nm NPs respectively, showing again that the 100 nm NPs
197 produced more toxicity than the 50 nm NPs on a particle amount basis.

198 The influence of NPs on the viscosity in hydra tissues was examined (Figure 3) and found to
199 increase in hydra extracts for both NPs sizes. For the 50 nm NPs, the viscosity increased in a
200 concentration dependent manner at concentrations > 2.5 mg/L. Viscosity persisted following the
201 24h depuration period with a significant increase at 2.5 mg/L. Correlation analysis revealed that
202 viscosity was significantly correlated with biomass (r=-0.56) and NPs in tissues (r=0.60) (Table
203 2). For the 100 nm, we obtained a peculiar bell-shaped response curve with an increase in viscosity
204 at low concentrations up to 2.5 mg/L NPs followed by a decrease at the higher concentrations. The
205 increased viscosity persisted after 24h depuration period with a significant increase at 5 mg/L
206 compared to controls. The formation of lipid-like LCs was examined using fluorescence
207 polarization spectroscopy (Figure 4). In hydra exposed to 50 nm NPs, a significant increase in
208 polarization was observed at the highest concentration tested (80 mg/L). There was no significant
209 increase in polarization after the 24h depuration period. In hydra exposed to the 100 nm NPs, a
210 significant increase in polarization was found at concentrations > 2.5 mg/L. Increased polarization
211 persisted after the 24h depuration period at 5 mg/L. Correlation analysis revealed that LCs
212 formation (polarisation) was significantly correlated with total lipids (r= 0.40) and NPs in tissues
213 (r=0.46) (Table 2). Changes in levels of polar lipids and LPO were also studied in hydra exposed
214 to the NPs (Figure 5A to 4D). In hydra exposed to 50 nm NPs, the levels of polar lipids were
215 significantly increased at concentrations between 5 and 80 mg/L (Figure 5A). The lipids levels
216 returned to control values after the 24h depuration period. The levels of LPO followed a biphasic
217 response where the levels were increased at low concentrations (1.25 to 5 mg/L) followed by a
218 decrease at higher concentrations where morphological effects were observed (Figure 5B). After

the 24h depuration period, LPO levels in controls were higher than the 96h control but the levels returned to control values at 5 mg/L. In hydra exposed to the 100 nm NPs, the polar lipids levels were significantly increased at concentrations ≥ 5 mg/L with the exception of the 40 mg/L owing to data variability (Figure 5C). This effect persisted for the 5 mg/L treatment after the 24h depuration period. Lipids levels were significantly correlated with viscosity (r=0.59) (Table 2). LPO levels were significantly increased at concentrations ≥ 2.5 mg/L in respect to controls (Figure 5D). Oxidative stress persisted after the 24h depuration period with the 1.25 and 5 mg/L NP concentration.

In the attempt to gain a global view on the effects of NPs on hydra, a principal component analysis was performed on the 50 and 100 nm diameter NPs (Figure 6). In hydra exposed to the 50 nm NPs, 62 % of the total extracted variance was obtained with the biomarkers used in the present study (Figure 6A). The most significant biomarkers were NPs levels in tissues (exposure), viscosity, LCs and polar lipids (biomarkers of effects). Tissue levels of NP were closely related with lipids and changes in viscosity. In hydra exposed to the more toxic 100 nm NPs, 60% of the total variance was explained by the endpoints used in the study (Figure 6B), with NP, LCs formation, LPO and viscosity changes being the most important biomarkers. NPs in tissues were closely related with LPO, lipids levels and LC formation but weakly associated with viscosity. Lipids levels and the formation of organized LCs where closely associated with each other which suggests that toxicity involves the formation of organized (anisotropic) LCs in hydra exposed to NPs.

Discussion

The 100 nm diameter NP was 1.7 times more toxic than the 50 nm diameter NP on a particle concentration basis. The EC50 for morphological changes was 3.6 and 18 mg/L for the 50 and 100 nm NPs respectively which was in the same range of the LC50 values (4.8 and 8.9 mg/L for 70

and 100 nm diameter NPs) for *Artemia salina* shrimp exposed to the polystyrene NPs in saline waters (Mishra et al., 2019). In this study the smaller NPs showed more toxicity on a mass basis than the larger ones as observed in *Hydra attenuata* but the equivalent amount of particles was not provided. NPs produced oxidative stress as determined by LPO expression in hydra, which were also induced in *Artemia*, corroborating our findings that polystyrene NPs produce oxidative damage. Although oxidative stress (LPO) was involved in hydra exposed to the NPs, LPO levels were more closely associated with levels of the 100 nm diameter NP than the 50 nm NP based on principal component analysis. This could be explained by the observation of hydra losing their tentacles at high concentrations of NPs potentially contributing to the variability in the levels of internal NPs and oxidative stress. This is consistent with the peculiar bell-shaped response obtained for LPO in hydra exposed to the 50 nm NPs. Oxidative stress was also observed in acs-22 mutant *Caernorhabditis elegans* (nematodes) exposed to polystyrene NPs (Qu et al., 2018). The NPs dysregulated some of the genes involved in the control of oxidative stress and activated the expression of Nrf signaling which governs the antioxidant response pathway. In another study with *C. elegans*, the uptake of 50 and 200 nm polystyrene NPs induced changes in metabolic profiles and toxicity (Kim et al., 2019). The uptake of these NPs lead to perturbation in energy metabolism (glucose and lactate) with induction of oxidative stress leading to reductions in locomotion and reproduction. These observations are consistent with the present study were reduction in tentacles and biomass were observed in hydra exposed to the NPs. In *Daphnia pulex*, polystyrene NPs induced stress defence and immobilization during a 21-day exposure regime (Liu et al., 2019). Indeed, as the fluorescent NP increased in the water fleas, genes involved in antioxidant pathways (superoxide dismutase, catalase and glutathione S-transferase) initially increased, followed by a decrease in gene expression. In zebrafish embryos, smaller-size

polystyrene NPs accumulated in lipid-rich regions such as in the egg yolk sac (Lee et al., 2019). Oxidative stress and inflammation were also observed in zebrafish embryos exposed to the NPs. This is consistent with the increase in polar lipids in hydra exposed to the NPs where the NPs in tissues were significantly correlated with polar lipids, viscosity and the formation of organized lipid-like LCs. This suggests that NPs could mobilize lipids into forming organized liquid crystal and perhaps increasing oxidative damage in cells. The mobilization of lipids could also result from the decreasing in hydra biomass (decrease in energy). For the 50 nm NPs, an analysis of covariance of lipids levels with biomass as the covariate revealed that both the exposure concentration ($p=0.002$) and biomass reduction ($p=0.02$) were significant, suggesting that both processes occurred where the concentration of NPs was higher. In the case of 100 nm NPs, covariance analysis revealed that the exposure concentration significantly influenced lipid levels with loss of biomass having no significant effect. This suggests that lipids were mobilized in respect to NPs exposure where a loss of biomass (fasting effect) had little influence on lipid contents in hydra.

The introduction of hydrophobic NPs such as polystyrene in cells could disrupt the conformational changes of proteins and lipid organisation in the cytoplasm. For example in zebrafish embryos exposed to NPs, the nanoparticles partitioned in lipid-rich environment of the yolk sac and induced the expression of protein chaperones: heat shock proteins 70 and 90 (Kim et al., 2019). Interestingly, the more toxic 100 nm NP revealed that NP in tissues were more closely associated with organized lipid-like LCs and LPO in hydra. The FOE probe for LCs evaluation is composed of an aliphatic carbon chain with a polar head (fluorescein) which can interact in hydrophobic environments (lipid-like) which polarize fluorescence. Preliminary experiments revealed that NPs alone do not significantly influence polarization but when combined with the post-mitochondrial fraction, polarization occurs (Gagné et al., 2019a). It was proposed that fluorescence polarization

occurs at the lipid/protein corona of the NPs given the hydrophobic nature of the FOE probe.The formation of lipid corona in addition to protein corona was also reported with other nanoparticles such as colloidal gold (Zhang et al., 2018). Although the formation of lipid corona on gold nanoparticles was governed by electrostatic interactions (cations at the surface proving better to attract lipids than anionic charged nanoparticles), hydrophobic interactions could also induce organized structures on the surface of polystyrene NPs (Gagné et al., 2019). In another study, oleic acid-coated iron oxide nanoparticles were also toxic to neuronal cells (Fernandez-Bertolez et al., 2018). Although the coated iron oxide nanoparticles were moderately toxic to cells, the compound was able to produce single stranded DNA damage and reduced DNA repair activity in the presence of H_2O_2 (oxidative stress). In human astrocytes, exposure to oleic acid-coated iron oxide nanoparticles was also genotoxic, inducing primary DNA damage as determined by the comet assay (Fernandez-Bertolez et al., 2019). However, the damage was seemingly reversible given that no permanent cytogenetic damage (micronuclei) was observed. In conclusion, polystyrene NPs were bioavailable to hydra and persisted after a 24 h depuration period. The 100 nm NPs was more toxic than the 50 nm NP when compared on particle concentration basis. Toxicity was dependent on the interaction between NP levels in hydra, lipids, the formation of organized LCs and oxidative stress. The mobilization of lipids by the NPs could represent a mechanism for the elimination of NPs from cells but could increase the toxicity (bioactivation) of NPs during this process.

Acknowledgements. The authors thank Pascale Bouchard from the Quebec Bioanalytical Laboratory of Environment and Climate Change Canada for performing the hydra exposure tests.

References

Al-Salem S, Lettieri P., Baeyens J. Recycling and recovery routes of plastic solid waste (PSW): a review**.** Waste Manag. 29: 2625-2643, 2009.

Blaise, C., Kusui, T. Acute toxicity assessment of industrial effluents with a microplate-based *Hydra attenuata* assay. Environ. Toxicol. Water Qual. 12: 53–60, 1997.

Bradford, M.M. A rapid and sensitive method for the quantitation of microgram quantities of protein utilizing the principle of protein-dye binding. Anal. Biochem. 72: 248–254, 1976.

Colvin VL, Kulinowski KM, Nanoparticles as catalysts for protein fibrillation. PNAS 104: 8679–8680, 2007.

Fernández-Bertólez N, Costa C, Brandão F, Kiliç G, Teixeira JP, Pásaro E, Laffon BV. Neurotoxicity assessment of oleic acid-coated iron oxide nanoparticles in SH-SY5Y cells. Toxicology 406-407 : 81-91. 2018.

Fernández-Bertólez N, Costa C, Brandão F, Duarte JA, Teixeira JP, Pásaro E, Valdiglesias V, Laffon B. Evaluation of cytotoxicity and genotoxicity induced by oleic acid-coated iron oxide nanoparticles in human astrocytes. Environ Mol Mutagen. In press, 2019.

Finney DJ. Statistical Methods in Biological Assay, 2nd ed. Griffin, London, England, 1964.

Gagné F. Oxidative stress, Chap 6. In: Biochemical Ecotoxicology: Principle and Methods, New York, Elsevier Inc. pp. 103-115, 2014.

Gagné F. Detection of polystyrene nanoplastics in biological tissues with a fluorescent molecular rotor probe**.** J. Xenobiotics 9: 8147-8149, 2019.

Gagné F, Auclair J, André C. Polystyrene nanoparticles induce anisotropic effects in subcellular fraction of the digestive system of freshwater mussels. Curr. Top. Toxicol. 15: 43-49, 2019a.

Gagné, F., Auclair, J., Quinn, B. Detection of polystryrene nanoplastics in biological samples based on the solvatochromic properties of Nile Red: application in *Hydra attenuata* exposed to nanoplastics. Environ. Sci. Poll. Res.: 2019b.

Greenspan P, Fowler SD. Spectrofluorometric studies of the lipid probe, Nile red. J Lipid Res. 26: 781-978, 1985.

Kim HM, Lee DK, Long NP, Kwon SW, Park JH. Uptake of nanopolystyrene particles induces distinct metabolic profiles and toxic effects in *Caenorhabditis elegans*. Environ. Pollut. 246: 578-586, 2019.

Haidekker MA, LingT, Anglo M, Stevens HY, Frangos JA, Theodorakis EA. New fluorescent probes for the measurement of cell membrane viscosity. Chemistry & Biology 8: 123-131, 2001.

Ho BT, Roberts TK, Lucas S. An overview on biodegradation of polystyrene and modified polystyrene: the microbial approach**.** Crit. Rev. Biotechnol. 38: 308-320, , 2018.

Lambert S, Wagner M. Characterisation of nanoplastics during the degradation of polystyrene. Chemosphere 145: 265-268, 2016.

Lee WS , Cho HJ , Kim E , Huh YH , Kim HJ , Kim B , Kang T , Lee JS , Jeong J . Bioaccumulation of polystyrene nanoplastics and their effect on the toxicity of Au ions in zebrafish embryos. Nanoscale 11: 3173-3185, 2019.

Liu Z, Yu P, Cai M, Wu D, Zhang M, Huang Y, Zhao Y. Polystyrene nanoplastic exposure induces immobilization, reproduction, and stress defense in the freshwater cladoceran *Daphnia pulex*. Chemosphere 215: 74-81, 2019.

Mishra P, Vinayagam S, Duraisamy K, Patil SR, Godbole J, Mohan A, Mukherjee A, Chandrasekaran N. Distinctive impact of polystyrene nano-spherules as an emergent pollutant toward the environment. Environ Sci Pollut Res Int. 26: 1537-1547, 2019.

Murphy, F., Quinn, B. The effects of microplastic on freshwater *Hydra attenuata* feeding, morphology & reproduction. Environ. Poll. 234: 487-494, 2018.

Qu M, Xu K, Li Y, Wong G, Wang D. Using acs-22 mutant *Caenorhabditis elegans* to detect the toxicity of nanopolystyrene particles. STOTEN 643: 119-126, 2018.

Pascoe D, Karntanut W, Müller CT. Do pharmaceuticals affect freshwater invertebrates? A study with the cnidarian Hydra vulgaris. Chemosphere 51: 521-5238, 2003.

Quinn B, Gagné F, Blaise C. Hydra, a model system for environmental studies. Int. J. Dev. Biol. 56: 613-625, 2012.

Verschoor A, ban Herwijnen R, Postuma C, Klesse K., Werner S: Assessment document of land-based inputs of microplastics in the marine environment. Environmental Impact of human activities Series, OSPAR 2017; https://www.ospar.org/documents?v=38018

Wang F, Bexiga MG, Anguissola S, Boya P, Simpson JC, Salvati A, Dawson KA, Time resolved study of cell death mechanisms induced by amine-modified polystyrene nanoparticles. Nanoscale 5: 10868-10876, 2013.

Wilby OK. The Hydra regeneration assay. In: Proceedings of the Workshop Organised by Association Francaise de Teratologie. pp. 108–124, 1989.

Zhang X, Pandiakumar AK, Hamers RJ, Murphy CJ. Quantification of Lipid Corona Formation on Colloidal Nanoparticles from Lipid Vesicles. Anal. Chem. 90: 14387-14394, 2018.

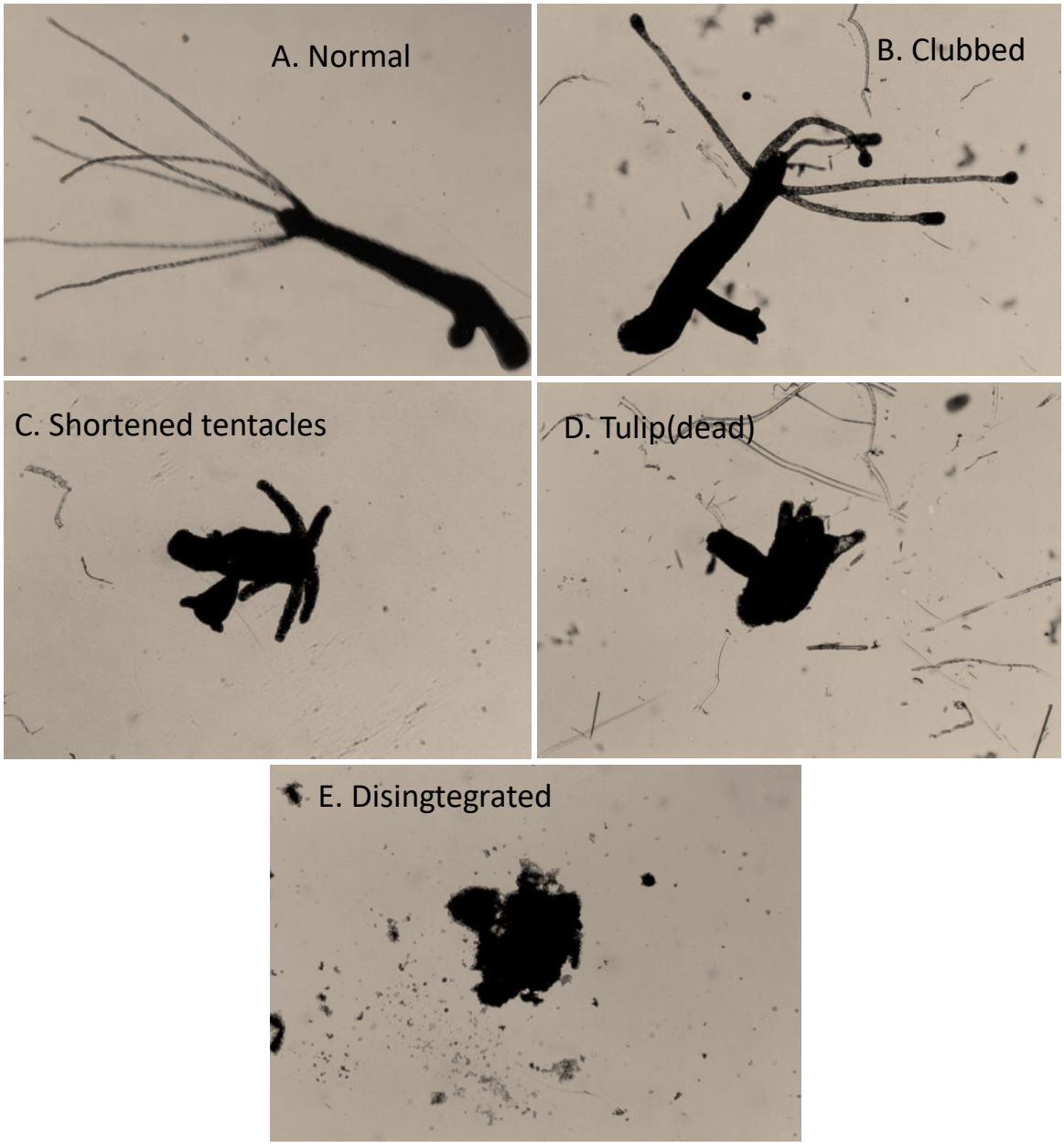

Figure 1. Morphological stages in *Hydra attenuate* after exposure to REEs for 96h (magnification x40): healthy polyp (A); clubbed tentacles (B); shortened tentacles(C); tulip stages (D) and disintegrated stage (E).

A 50 nm NP

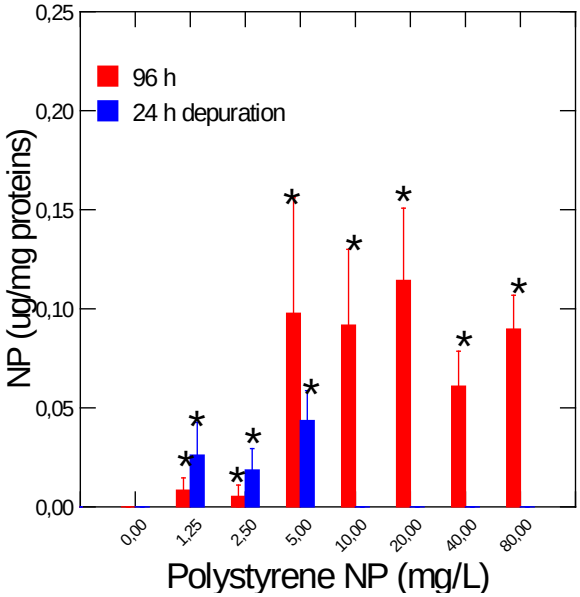

B 100 nm NP

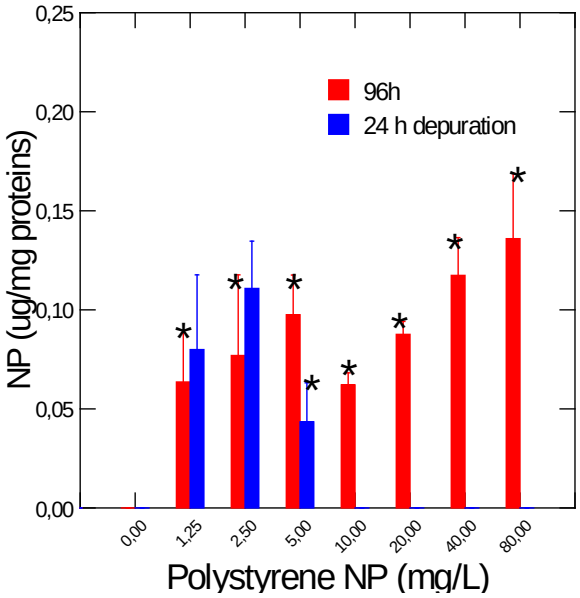

Figure 2. Detection of NP in *Hydra attenuata* using a molecular rotor probe.
Hydra were exposed to increasing concentrations of 50 nm (A) and 100 nm (B) polystyrene nanoplastics for 96 h at 20ºC. A subset of organisms were placed in clean media for 24 h for depuration. The data represent the mean with the standard error. The star * symbol indicated significance from controls (0) at $p<0.05$.

A 50 nm NPs

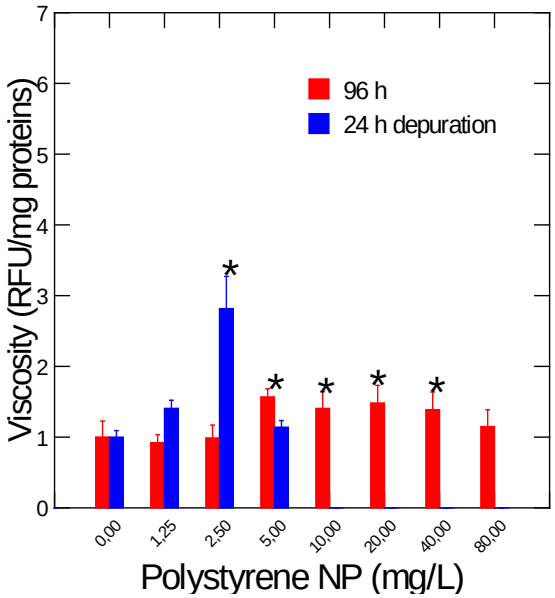

B 100 nm NPs

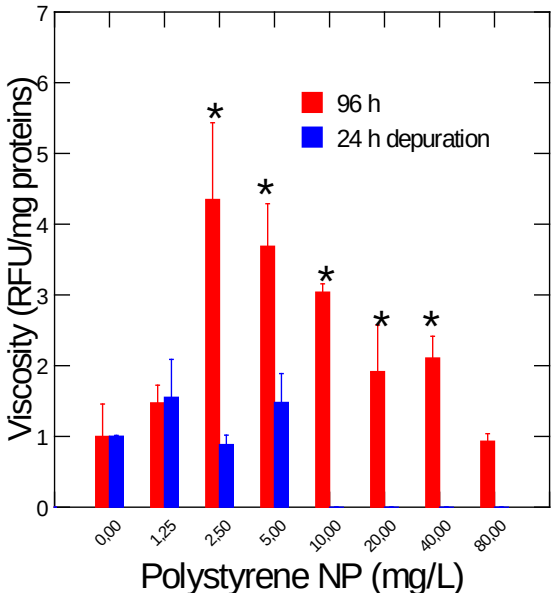

Figure 3. Change in viscosity in *Hydra attenuata* tissues exposed to NPs
Hydra were exposed to increasing concentrations of 50 nm (A) and 100 nm (B) polystyrene nanoplastics for 96 h at 20°C. A subset of organisms were placed in clean media for 24 h for depuration. The data represent the mean with the standard error. The star * symbol indicated significance from controls at $p<0.05$.

A 50 nm NPs

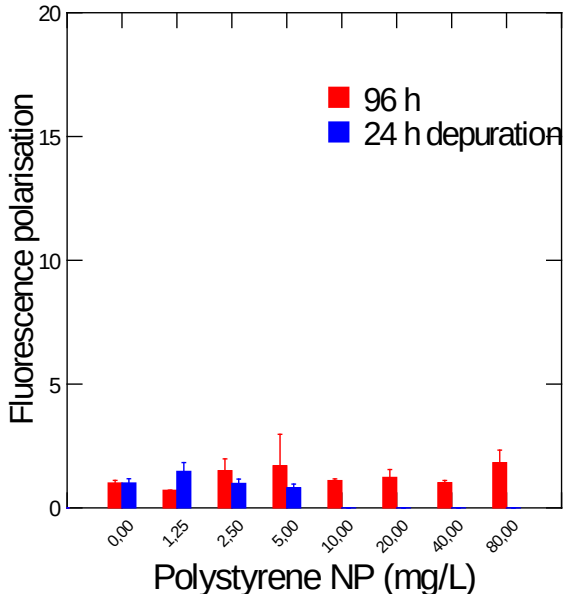

B 100 nm NPs

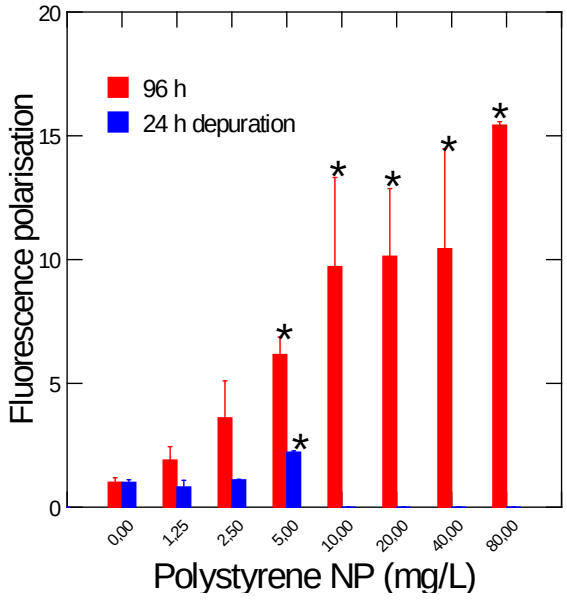

Figure 4. Formation of lipid-like liquid crystals in *Hydra attenuata* exposed to NPs. Hydra were exposed to increasing concentrations of 50 nm (A) and 100 nm (B) polystyrene nanoplastics for 96 h at 20°C. A sub-set of organisms were placed in clean media for 24 h for depuration. The data represent the mean with the standard error.The star * symbol indicated significance from controls (0) at $p<0.05$.

A 50 nm NPs

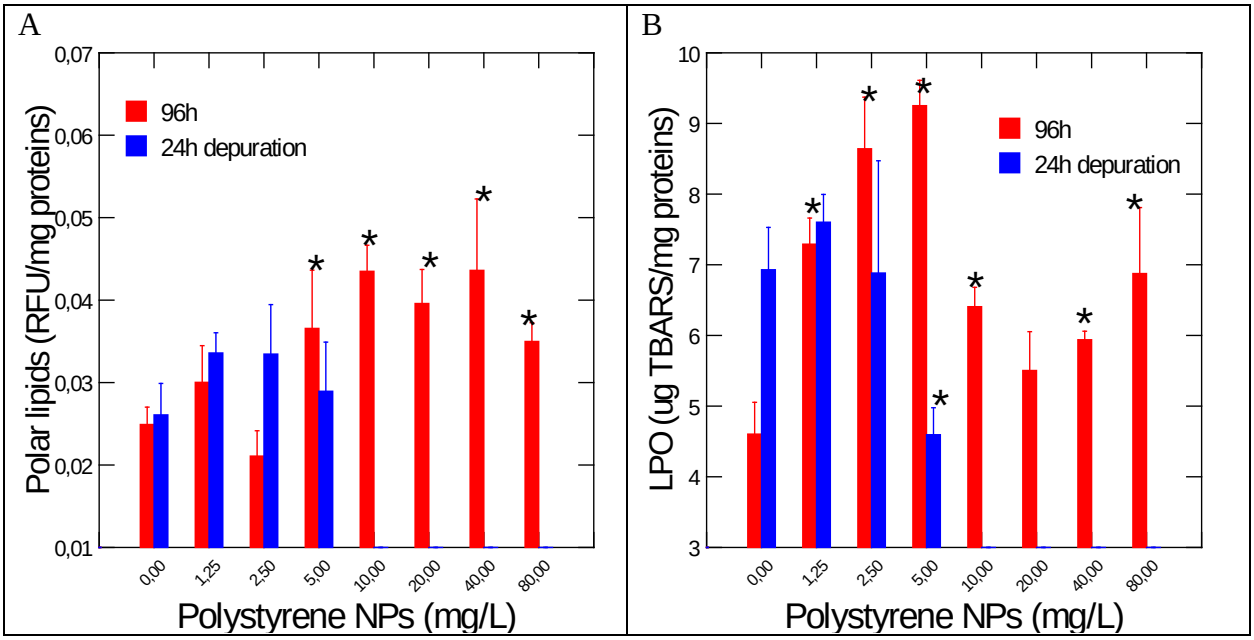

B 100 nm NPs

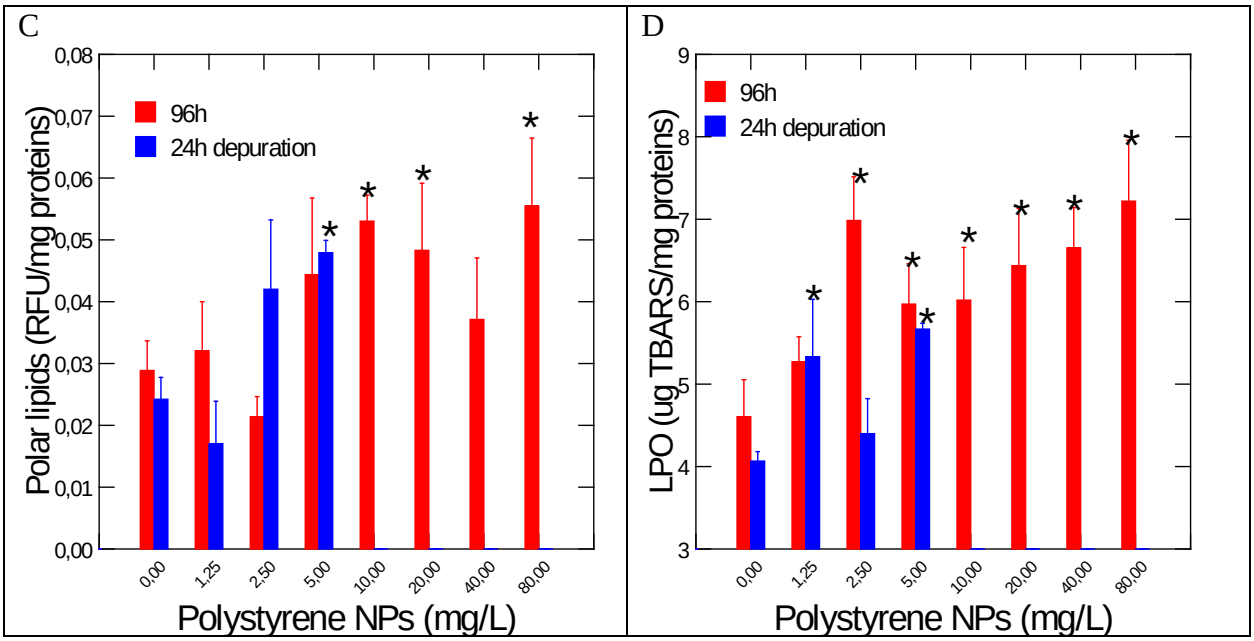

Figure 5. Changes in lipid contents and oxidative stress in *Hydra attenuata* exposed to NPs

Hydra were exposed to increasing concentrations of 50 nm (A) and 100 nm (B) polystyrene nanoplastics for 96 h at 20ºC. A subset of organisms were placed in clean media for 24 h for depuration. The data represent the mean with the standard error. The star * symbol indicated significance from controls (0) at $p<0.05$.

468

469 A 50 nm NPs

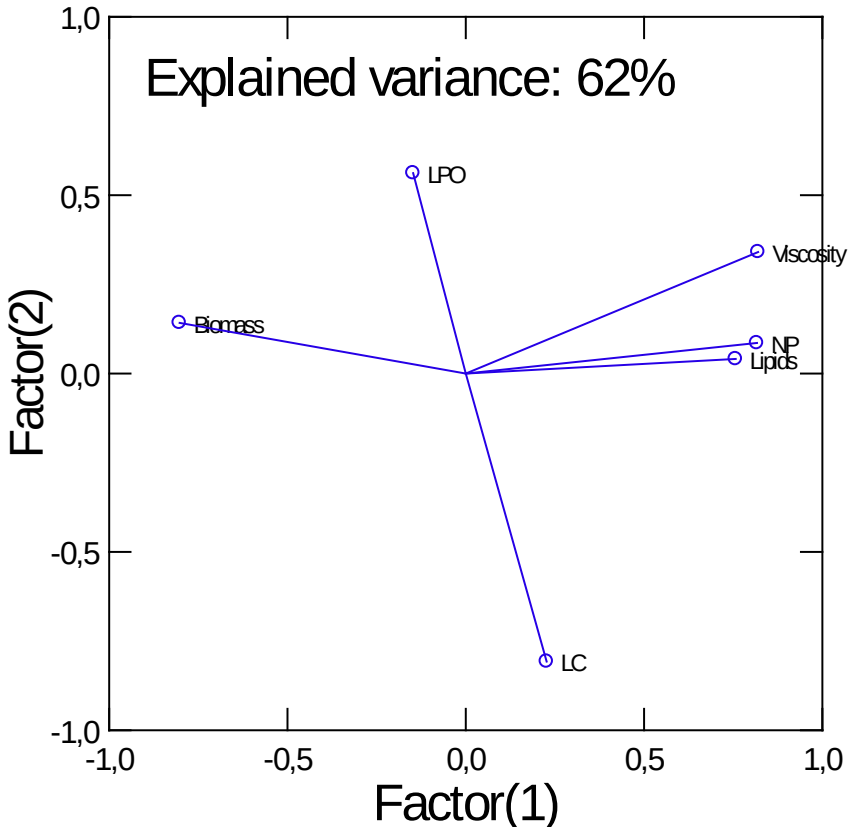

470

471

472 100 nm NPs

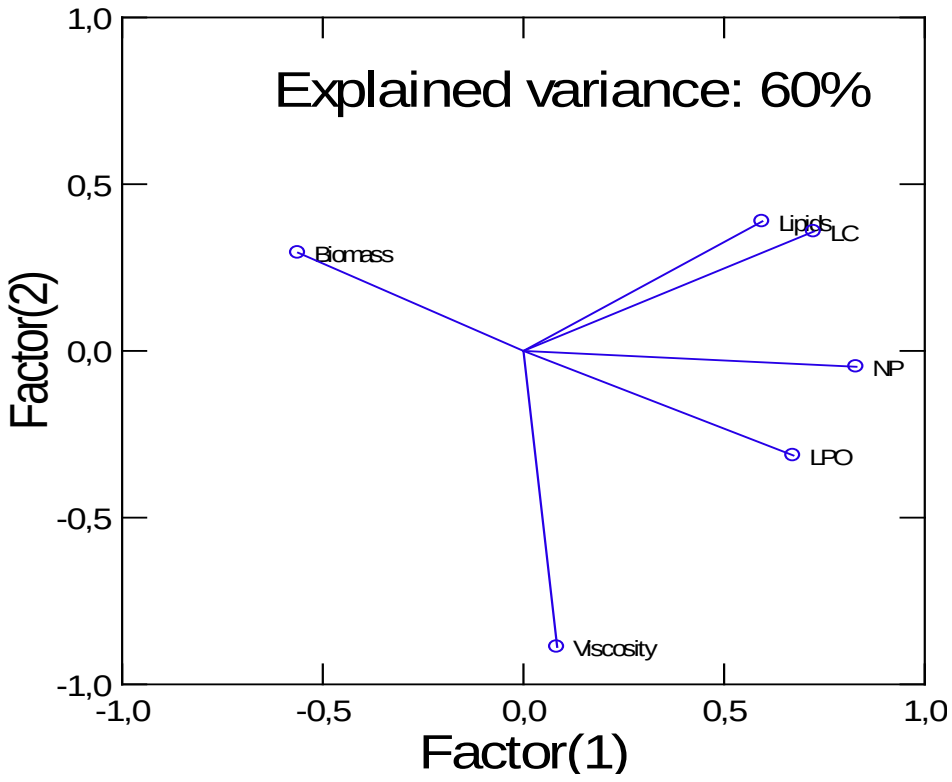

473

474 Figure 6. Factorial analysis of biomarker data in *Hydra attenuata* exposed to 50 nm (A) and 100
475 nm (B) NPs.The biomarker responses were analyzed using principal component analysis.
476

Table 1. Toxicity data of *Hydra attenuata* exposed to 50 and 100 nm polystyrene NPs

NP	LC50 in mg/L (95% confidence)	EC50 in mg/L (95% confidence)	Biomass[1] (EC50)	Observation
50 nm	> 80 mg/L	3.6 (3-4.7)	14 mg/L	White deposits on antennae at >5 mg/L
100 nm	> 80 mg/L	18.4 (14-25)	28 mg/L	White deposits on antennae at >5 mg/L

1. Concentration that decrease the turbidity at 600 nm of hydra homogenates by 50 %.

Table 2. Correlation analysis Table 1. Toxicity data of Hydra attenuata exposed to 50 and 100 nm polystyrene NPs

50 nm NP	Biomass	Lipids	NPs	Viscosity	LC	LPO
Biomass	1					
Lipids	**-0.38**	1				
NP	**-0.59**	**0.49**	1			
Viscosity	**-0.56**	**0.59**	**0.60**	1		
LC	-0.31	0.09	0.09	-0.04	1	
LPO	0.03	-0.20	-0.08	0.03	-0.08	1

100 nm NP	Biomass	Lipids	NPs	Viscosity	LC	LPO
Biomass	1					
Lipids	-0.18	1				
NP	**-0.44**	0.33	1			
Viscosity	-0.18	-0.10	0.02	1		
LC	-0.23	**0.40**	**0.46**	-0.15	1	
LPO	-0.15	0.21	**0.50**	0.25	**0.35**	1

Significant correlations ($p<0.05$) are highlighted in **bold.** NP: Nanoplastics in hydra, LC: liquid crystals (fluorescence polarisation), LPO: lipid peroxidation.